Original Article

Evaluation of ganglion cell-inner plexiform layer thickness in the diagnosis of preperimetric glaucoma and comparison to retinal nerve fiber layer

Gunjan A Deshpande, Richa Gupta, Prashant Bawankule[1], Dhananjay Raje[2], Moumita Chakraborty[2]

Purpose: The aim of this study was to evaluate the diagnostic ability of optic nerve head (ONH), RNFL, and GC-IPL parameters in differentiating eyes with PPG from normals. **Methods:** This was a retrospective, cross-sectional, observational study. We studied 73 eyes of 41 patients and compared them to 65 eyes of 34 normal persons. Each patient underwent detailed ocular examination, standard automated perimetry, GC-IPL, ONH, and RNFL analysis. PPG was defined as eyes with normal visual field results and one or more localized RNFL defects that were associated with a glaucomatous disc appearance (e.g., notching or thinning of neuroretinal rim) and IOP more than 21 mm Hg. Diagnostic abilities of GC-IPL, ONH, and RNFL parameters were computed using area under receiver-operating curve (AUROC), sensitivity and specificity, and likelihood ratios (LRs). **Results:** All GC-IPL parameters differed significantly from normal. The ONH, RNFL, and GC-IPL parameters with best area under curves (AUCs) to differentiate PPG were vertical cup to disc ratio (0.76), inferior quadrant RNFL thickness (0.79), and inferotemporal quadrant GC-IPL thickness (0.73), respectively. Similarly, best LRs were found for clock hour 5, 6, and 12 thicknesses among RNFL; inferior sector and inferotemporal sector thicknesses among GC-IPL parameters. **Conclusion:** Diagnostic abilities of GC-IPL parameters were comparable to RNFL parameters in differentiating PPG patients from normals. The likelihood of ruling in a disease was greater with GC-IPL parameters.

Access this article online

Website: www.ijo.in

DOI: 10.4103/ijo.IJO_965_20

Quick Response Code:

Key words: Ganglion cell-inner plexiform layer, preperimetric glaucoma, retinal nerve fiber layer

Glaucoma is the leading cause of irreversible blindness worldwide by virtue of loss of retinal ganglion cells (RGCs), leading to classic optic nerve head (ONH) changes and visual field (VF) defects.[1,2] The early detection of glaucoma is of paramount importance to retard disease progression and preserve maximum vision. It has been reported that a proportion of glaucomatous eyes show structural changes in only the retinal nerve fiber layer (RNFL) and/or ONH, without any apparent defect in visual function.[3,4] The term 'preperimetric glaucoma' (PPG) has been used to describe eyes with a glaucomatous optic disc and/or fundus appearance and an apparently normal VF.[3]

Optical coherence tomography (OCT) is a reliable diagnostic modality used to detect glaucoma. It is widely used for structural evaluation of glaucomatous eyes.[5] With the introduction of spectral-domain OCT (SD-OCT), retinal imaging has been facilitated at higher resolution. Software versions 6.0 or higher of Cirrus High-Definition OCT (Carl Zeiss Meditech, Dublin, California) now provide a ganglion cell analysis in which GCL/IPL thickness measurements are provided.[6]

Recently published data suggest that evidence of glaucomatous damage can be observed in the inner retina or ganglion cell complex (GCC), early during the disease process by means of SD-OCT.[7] Lisboa *et al*. found that GCC loss could be detected in eyes with PPG.[8] As >50% of all RGCs are concentrated and multilayered in the macular area, macular thickness parameters can be used as complementary methods.[5]

Department of Glaucoma, Sarakshi Netralaya, Nagpur, [1]Department of Retina, Sarakshi Netralaya, [2]Department of Data Analysis, MDS Bioanalytics, Nagpur, Maharashtra, India

Correspondence to: Dr. Gunjan A Deshpande, Department of Glaucoma, Sarakshi Netralaya, Nagpur, Maharashtra, India. E-mail: drgunjandeshpande@gmail.com

Received: 13-Apr-2020 Revision: 02-Oct-2020
Accepted: 12-Dec-2020 Published: 30-Apr-2021

To the best of our knowledge, the GC-IPL evaluation in PPG in Indian population can be found in two studies (Begum *et al*. and Kaushik *et al*.).[9,10] The diagnostic ability of GCIPL parameters was significantly lower than that of ONH and RNFL parameters in the former and GC-IPL evaluation did not outperform RNFL measurements in PPG in the latter. Interestingly, we found that the likelihood of ruling in a disease was greater with GC-IPL parameters in contrast to the earlier two studies. We are herewith reporting our findings of evaluation of the diagnostic ability of GC-IPL, ONH, and RNFL structural parameters in PPG eyes in Indian population.

Methods

This was a retrospective, observational, cross-sectional study performed at a tertiary care ophthalmology center. Data were collected and analyzed from consecutive patients who presented between December 2015 and May 2018 and satisfied the inclusion criteria. The study was approved by the Hospital Ethics Committee and adhered to the declaration of Helsinki. All the patients underwent a medical history review, detailed ocular examination including visual acuity, cycloplegic refraction, slit-lamp examination, indirect ophthalmoscopy, intraocular pressure (IOP) with Goldmann's Applanation Tonometer, 4 mirror indentation gonioscopy with Sussman's

Cite this article as: Deshpande GA, Gupta R, Bawankule P, Raje D, Chakraborty M. Evaluation of ganglion cell-inner plexiform layer thickness in the diagnosis of preperimetric glaucoma and comparison to retinal nerve fiber layer. Indian J Ophthalmol 2021;69:1113-9.

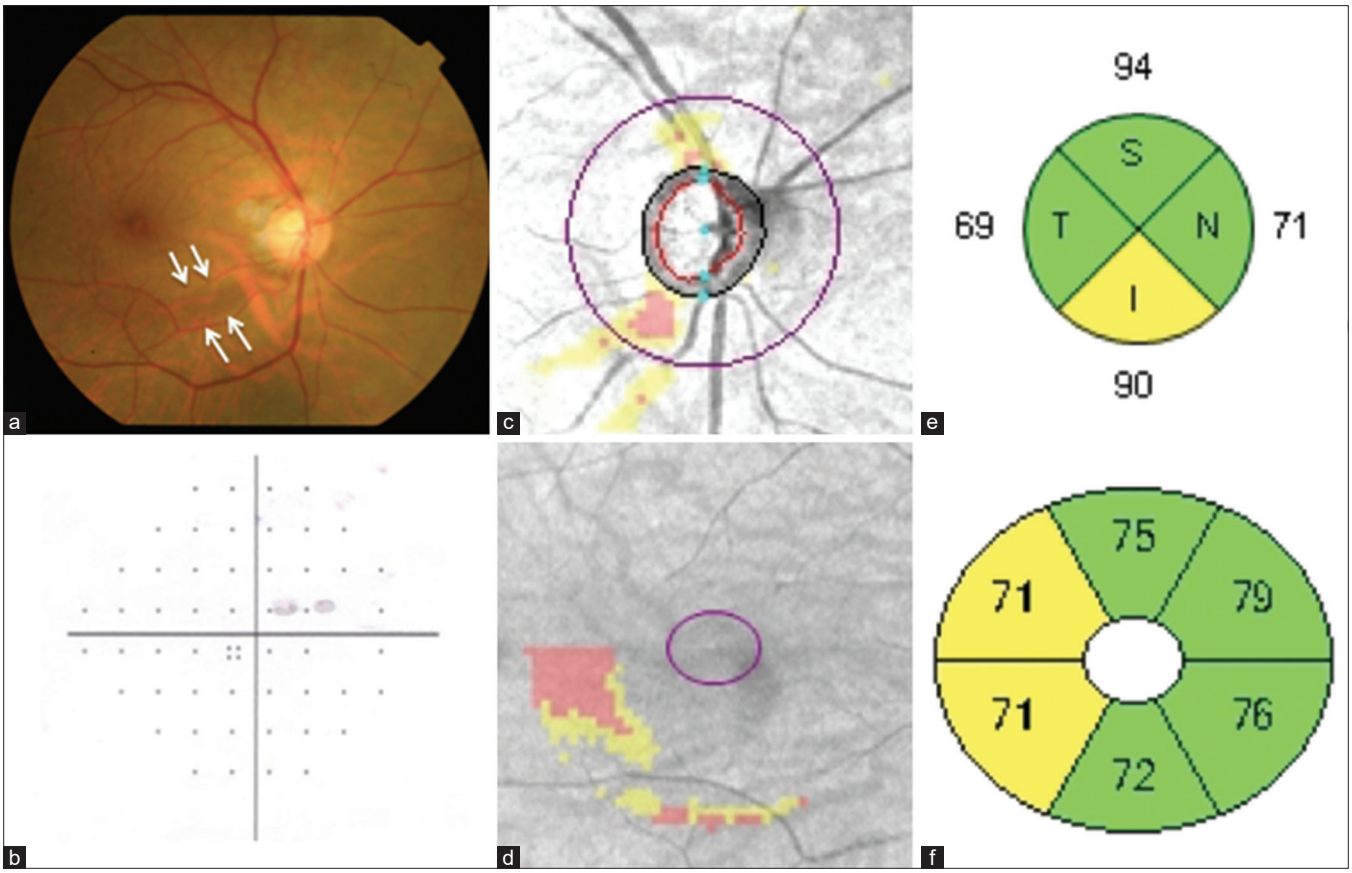

Figure 1: A 40-year-old man in the preperimetric glaucoma group. (a) Fundus photography showing localized RNFL defect. (b) Normal visual field on automated perimetry. (c and d) Peripapillary RNFL and GC-IPL deviation maps showing thinning in inferior region. (e and f) Defects on RNFL quadrant and GC-IPL sector analysis

Gonioscope, ONH evaluation with slit-lamp biomicroscopy using 78D noncontact lens. VFs were mapped using Humphrey Visual Field Analyzer (Carl Zeiss Meditec, Dublin, California) with the 24-2 Swedish Interactive Threshold Algorithm [SITA] standard program, and spectral-domain OCT (SD-OCT) examinations were performed with Cirrus SD-OCT, (Carl Zeiss Meditec, Dublin, California)

The inclusion criteria of the study were as follows: age more than 18 years, best-corrected visual acuity of Snellens >6/12 (logMAR <0.3), refractive error (under cycloplegia) between –6 dioptre sphere (DS) myopia, +4 DS hyperopia, and ±3 DS of astigmatism, open angles on indentation gonioscopy, standard automated perimetry (SAP) test with reliable indices. VF results were considered reliable if fixation losses, false-positive and false-negative values were <15% after two consecutive tests. The SD-OCT with signal strength age were included. Images with lost data on the peripapillary ring, motion artefact, or incorrect segmentation were excluded from the study. The patients with media opacity, history of trauma and intraocular surgery, macular pathology, previous laser therapy, and neurologic disease that could affect the VFs were also excluded.

PPG was defined as eyes with normal VF results and one or more localized RNFL defects that were associated with a glaucomatous disc appearance (e.g., focal or diffuse RNFL thinning, notching, or thinning of neuroretinal rim) and IOP more than 21 mm Hg. Normals were eyes with no history of ocular disease, an IOP of ≤21 mmHg, a normal appearing optic disc, SAP within normal limits, and normal OCT [Fig. 1]. All the eyes were evaluated clinically by two glaucoma experts, who were masked to the VF and SDOCT results. All the eyes were divided into PPG and normal groups after consensus between the experts. Eyes which could not be classified into either glaucomatous or normal groups and created inconsistencies between the experts were excluded.

OCT procedure

The Optic Disc Cube 200*200 consisted of 40,000 axial scans (in a 6 mm × 6 mm × 2 mm cube) centered on the optic disc. Average RNFL thickness and RNFL thickness in quadrants on a measurement circle 3.46 mm in diameter were calculated, and their deviation from a normative database was provided in a color-coded scheme. The RNFL pseudocolor thickness maps and deviation maps were also provided. The parameters identified were average RNFL thickness, rim area, disc area, average cup-disc ratio (CDR), vertical CDR, cup volume and superior, inferior, temporal, and nasal RNFL quadrant thicknesses.

The GC-IPL analysis available on the Cirrus software version 6.0 (or higher) measured the combined thickness of RNFL, GCL and IPL in a 4.8 mm × 4.0 mm oval with a longer horizontal axis. It provided measurements in 6 wedge-shaped sectors after excluding the central foveolar region (1 mm in diameter) along with a pseudocolor scheme for the GC-IPL thickness. A deviation map also flagged abnormally thin areas as yellow ($P < 5\%$) or red ($P < 1\%$) superpixels. The parameters identified were average GC-IPL, minimum GC-IPL, and

sector measurements (superonasal, superior, superotemporal, inferonasal, inferior, and inferotemporal).

Statistical analysis

The demographic characteristics were compared using Student's *t* test and Chi-square test, respectively. Descriptive statistics included mean and standard deviation for continuous variables, and frequency distributions for categorical variables. Student's *t* test was used to compare signal strength, global, quadrant, and clock hour parameters. The measurements from both eyes of the same patients were likely to be correlated, and ignoring these inter-eye correlations would have impacted the variance estimators and significance values. Therefore, a linear mixed model was used to analyze such correlated data, containing both fixed and random effects. Here, age was considered as fixed effect while individuals as random effects. Predicted values for each ONH, RNFL, and GCIPL parameters were obtained using linear mixed model. The ability of the predicted values to distinguish between PPG and control eyes was evaluated using the area under receiver operating characteristics (AUROC) curves. The cut-off point for each parameter was obtained using the Youden index. The sensitivity and specificity for the cut-off value of parameters were obtained as indicators of diagnostic validity. The confidence intervals (CIs) for AUROC curve were computed with 1000 stratified bootstrap replicates. Likelihood ratios (LRs) for positive and result were obtained for each parameter and compared as:

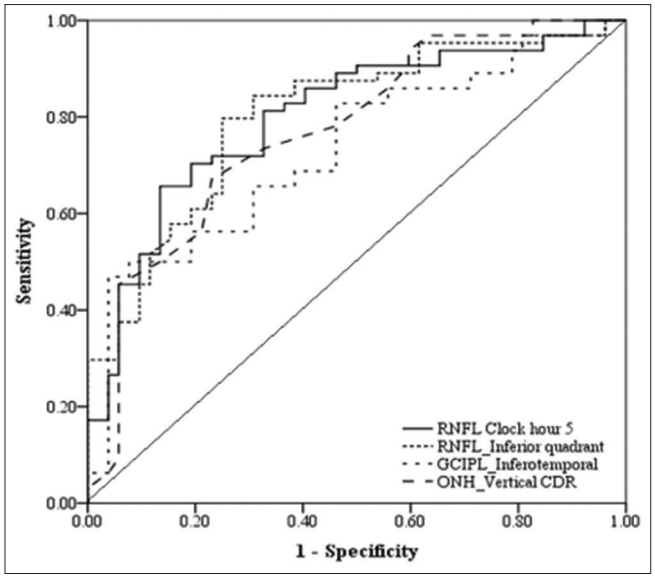

Figure 2: ROC curves for the four best diagnostic indicators of PPG based on AUCs

P: $LR^X+ > LR^Y+$
A: $LR^X- < LR^Y-$

Where X and Y were the two tests being compared. If the equivalence P holds true, then X is superior in confirming the presence of disease and if A holds true, then X is superior in confirming the absence of disease. If both P and A holds true, then X is overall superior to Y, and if both are violated, then X is inferior to Y. Accordingly, better diagnostic parameters were selected. The statistical analyses were performed using the R-3.3.0 (R Core Team 2016) programming tool and the statistical significance was tested at 5% level.

Results

On the basis of the optic disc imaging quality and reliability of VFs, 65 eyes of 34 control individuals and 73 eyes of 41 patients diagnosed with PPG were included. Table 1 provides the statistics for demographic characteristics of patients. The mean age of patients with PPG (58.29 ± 10.42 years) was higher than that of control group (54.06 ± 12.43 years); the difference was statistically insignificant. The gender distribution in two groups was also statistically insignificant. Table 2 shows that the differences between groups in ONH parameters like signal strength and disc area were statistically insignificant. The mean rim area was significantly higher in control eyes as compared to affected eyes (P = 0.0002). The average CDR, vertical CDR and cup volume were significantly higher in PPG eyes as compared to control eyes. Among RNFL parameters, nine out of 12 clock hour parameters were significantly different between two groups. Further, the means of superior, nasal, and inferior quadrant measurements in PPG were significantly smaller than that of control eyes. All the GC-IPL parameters were significantly smaller in PPG as compared to control group.

Initially, the diagnostic strength of ONH, RNFL, and GC-IPL was assessed in terms of AUC, sensitivity, and specificity, with the results shown in Table 3 and Fig. 2. Among ONH parameters, vertical and average CDR showed relatively higher AUC as compared to rim area and cup volume in discriminating control and PPG eyes. The sensitivity of average CDR was higher than and vertical CDR, whereas specificity of vertical CDR was higher than average CDR. Amongst all the ONH parameters, rim area had the maximum specificity in detecting PPG. Within RNFL parameters, the inferior quadrant had the maximum AUC followed by superior and nasal quadrants. The sensitivity of inferior and superior quadrants was higher than their respective specificity. Among GC-IPL parameters, inferotemporal quadrant had the maximum AUC followed by superonasal quadrant and average thickness. The specificity of inferotemporal and average thickness was much higher than their respective sensitivity. Based on the magnitudes of sensitivity and specificity, it was hard to decide the superiority of one parameter over other. Hence, positive and negative LRs were obtained for each parameter as shown in Table 4.

Table 1: Demographic profile of patients included in the study

Levels	Groups		*P*
	Control (*n*=34)	Preperimetric Glaucoma (*n*=41)	
Age in years [mean±SD]	54.06±12.43	58.29±10.42	0.1128 (NS)*
Gender [no. (%)]			
Men	18 (52.94)	23 (56.10)	0.9678 (NS)†
Women	16 (47.06)	18 (43.90)	

*Obtained using Student's *t*-test; †Obtained using Pearson's Chi-square test; NS: Non-Significant

Table 2: Comparison of age, ONH, RNFL, and GCIPL parameters in control and preperimetric glaucoma eyes

	Groups [Mean±SD]		*P**
	Control (*n*=65)	Preperimetric Glaucoma (*n*=73)	
ONH parameters			
Signal strength	5.80±0.40	5.88±0.33	0.2275 (NS)
Disc area, mm^2	2.26±0.53	2.36±0.51	0.2630 (NS)
Rim area, mm^2	1.20±0.19	1.07±0.21	0.0002 (S)
Average CDR	0.66±0.10	0.73±0.07	<0.0001 (HS)
Vertical CDR	0.62±0.10	0.70±0.07	<0.0001 (HS)
Cup volume, mm^3	0.42±0.31	0.53±0.25	0.0294 (S)
RNFL parameters			
Clock hour_1, µm	111.88±21.05	102.36±19.08	0.0061 (S)
Clock hour_2, µm	67.14±10.95	63.49±10.37	0.0467 (S)
Clock hour_3, µm	47.32±7.37	46.52±6.83	0.5079 (NS)
Clock hour_4, µm	59.85±12.26	57.72±10.06	0.2678 (NS)
Clock hour_5, µm	119.31±19.8	101.58±19.92	< 0.0001 (HS)
Clock hour_6, µm	126.02±21.18	109.53±22.29	< 0.0001 (HS)
Clock hour_7, µm	92.88±19.33	80.52±21.85	0.0006 (S)
Clock hour_8, µm	64.43±13.74	56.52±8.46	0.0001 (S)
Clock hour_9, µm	57.48±8.66	54.51±7.90	0.3771 (NS)
Clock hour_10, µm	83.26±14.72	73.96±12.8	0.0001 (S)
Clock hour_11, µm	98.65±20.5	85.75±17.35	0.0001 (S)
Clock hour_12, µm	118.94±19.66	103.95±25.17	0.0002 (S)
Temporal quadrant, µm	57.77±8.19	56.85±8.03	0.5069 (NS)
Superior quadrant, µm	110.94±12.07	99.74±14.97	<0.0001 (HS)
Nasal quadrant, µm	68.66±8.87	62.23±7.46	<0.0001 (HS)
Inferior quadrant, µm	112.32±13.13	97.78±17.17	<0.0001 (HS)
Average thickness, µm	87.42±7.53	85.90±6.07	0.2004 (NS)
GCIPL parameters			
Signal strength	6.06±0.46	6.01±0.70	0.6401 (NS)
Superotemporal quadrant, µm	76.95±7.1	73.68±7.27	0.0086 (S)
Superior quadrant, µm	80.26±7.47	75.73±8.47	0.0012 (S)
Superonasal quadrant, µm	82.85±6.11	77.6±8.28	0.0001 (S)
Inferonasal quadrant, µm	79.97±7.87	75.73±7.91	0.0020 (S)
Inferior quadrant, µm	76.97±9.69	72.56±8.72	0.0057 (S)
Inferotemporal quadrant, µm	77.85±8.99	72.55±8.47	0.0005 (S)
Average, µm	79.18±7.06	74.71±8.02	0.0007 (S)
Minimum, µm	73.51±11.6	69.49±11	0.0389 (S)

*Obtained using Student's *t* test; HS=Highly significant, S=Significant, NS=Nonsignificant

The global and the quadrant parameters were compared based on equivalence criteria, as stated in methods, to decide about their diagnostic superiority. The vertical CDR, average RNFL thickness, and average GC-IPL thickness were compared referring to LR+ and LR- values [Table 4]. The paired comparison revealed that average GC-IPL thickness had the maximum LR+ value. Its LR+ value (4.23) indicated a moderate increase in the posttest probability of PPG. Its LR- value was minimum indicating its superiority in diagnosing the absence of PPG. The LR- value for the parameter (0.19) indicated a moderate decrease in the posttest probability. The comparison of superior RNFL and superior GC-IPL revealed that LR+ for superior RNFL was higher than superior GC-IPL, whereas LR- for RNFL was smaller than GC-IPL, indicating overall better diagnostic strength of superior RNFL as compared to superior GC-IPL. The positive/negative LR values for superior RNFL showed a slight increase/decrease in the posttest probabilities. As regards the inferior quadrant, LR+ of GC-IPL (4.90) was higher than that of RNFL indicating the strength of inferior GC-IPL quadrant in diagnosing PPG with a moderate increase in the posttest probability. The inferotemporal GC-IPL quadrant also showed equally strong likelihood of detecting the presence of PPG. The LR- of RNFL (0.19) was smaller than that of GC-IPL, thereby indicating the strength of inferior RNFL quadrant in diagnosing the absence of disease with a moderate decrease in posttest probability.

Overall, considering the LR+ magnitudes, inferior GC-IPL as well as inferotemporal GC-IPL quadrant are strong indicators of PPG, whereas inferior RNFL and average thickness are the strong indicators of absence of the disease.

Table 3: AUCs, sensitivities, specificities (with 95% CI in parentheses) along with *P* values of ONH, RNFL, and GCIPL parameters

	Diagnostic indicators		
	AUC (95% CI)	Sensitivity (95% CI)	Specificity (95% CI)
ONH parameters			
Rim area	0.70 (0.62-0.79)	58.90 (47.62-70.19)	81.54 (72.11-90.97)
Average CDR	0.74 (0.65-0.82)	78.08 (68.59-87.57)	64.62 (52.99-76.24)
Vertical CDR	0.76 (0.68-0.84)	72.60 (62.37-82.83)	75.38 (64.91-85.86)
Cup volume	0.65 (0.56-0.75)	82.19 (73.42-90.97)	50.77 (38.62-62.92)
RNFL parameters			
Clock hour_1	0.66 (0.57-0.75)	61.64 (50.49-72.8)	69.23 (58.01-80.45)
Clock hour_2	0.59 (0.49-0.68)	35.62 (24.63-46.6)	83.08 (73.96-92.19)
Clock hour_3	0.55 (0.45-0.64)	26.03 (15.96-36.09)	90.77 (83.73-97.81)
Clock hour_4	0.55 (0.45-0.65)	58.90 (47.62-70.19)	56.25 (44.10-68.40)
Clock hour_5	0.78 (0.7-0.85)	72.60 (62.37-82.83)	78.46 (68.47-88.46)
Clock hour_6	0.76 (0.68-0.84)	61.64 (50.49-72.80)	83.08 (73.96-92.19)
Clock hour_7	0.73 (0.64-0.81)	69.86 (59.34-80.39)	72.31 (61.43-83.19)
Clock hour_8	0.68 (0.59-0.77)	87.67 (80.13-95.21)	49.23 (37.08-61.38)
Clock hour_9	0.62 (0.52-0.71)	56.16 (44.78-67.55)	69.23 (58.01-80.45)
Clock hour_10	0.72 (0.64-0.81)	83.56 (75.06-92.06)	55.38 (43.30-67.47)
Clock hour_11	0.73 (0.65-0.82)	69.86 (59.34-80.39)	69.23 (58.01-80.45)
Clock hour_12	0.73 (0.64-0.82)	65.75 (54.87-76.64)	80.00 (70.28-89.72)
Temporal quadrant	0.53 (0.43-0.62)	43.84 (32.45-55.22)	67.69 (56.32-79.06)
Superior quadrant	0.76 (0.68-0.84)	86.30 (78.41-94.19)	63.08 (51.34-74.81)
Nasal quadrant	0.73 (0.65-0.82)	79.45 (70.18-88.72)	64.62 (52.99-76.24)
Inferior quadrant	0.79 (0.72-0.87)	87.67 (80.13-95.21)	66.15 (54.65-77.66)
Average thickness	0.63 (0.52-0.74)	89.04 (81.88-96.21)	63.08 (51.34-74.81)
GCIPL parameters			
Superotemporal quadrant	0.67 (0.58-0.76)	47.95 (36.49-59.41)	84.62 (75.84-93.39)
Superior quadrant	0.68 (0.59-0.77)	65.75 (54.87-76.64)	69.23 (58.01-80.45)
Superonasal quadrant	0.71 (0.63-0.80)	63.01 (51.94-74.09)	75.38 (64.91-85.86)
Inferonasal quadrant	0.67 (0.58-0.76)	45.21 (33.79-56.62)	89.23 (81.69-96.77)
Inferior quadrant	0.68 (0.59-0.77)	45.21 (33.79-56.62)	90.77 (83.73-97.81)
Inferotemporal quadrant	0.73 (0.64-0.81)	47.95 (36.49-59.41)	90.77 (83.73-97.81)
Average thickness	0.69 (0.6-0.78)	52.05 (40.59-63.51)	87.69 (79.71-95.68)
Minimum thickness	0.65 (0.56-0.75)	54.79 (43.38-66.21)	78.46 (68.47-88.46)

AUC=Area under curve

Discussion

We undertook this study to evaluate the diagnostic capability of GC-IPL, ONH, and RNFL structural parameters in differentiating PPG from normal individuals. The distributions of age, gender, disc area, and signal strengths of macula and ONH scans were comparable between both the groups. In our study, the best AUCs were shown by clock hour 5 (0.78) and inferior quadrant (0.79) on RNFL, inferotemporal sector on GC-IPL (0.73), and vertical CDR (0.76) on ONH. Our AUCs are better than another Indian cohort where AUCs of the best parameters were found to be around 0.7 and sensitivities at a specificity of 95% were around 25%.[11] The difference could be attributed to the fact that these control group comprised of eyes, which were of glaucoma suspects on ocular examination and were later, found to be normal on imaging. The importance of incorporating glaucoma suspects as controls has been cited previously.[5] The global values on RNFL including superior quadrant, nasal quadrant and inferior quadrant fared better than clock hour values (5, 6, 7, 11, 12, 1). However, it is well known that averaging of thicknesses over quadrants can mask localized defects.[11] Corresponding sensitivities and specificities of the best performing parameters were also found to be low on both RNFL and GC-IPL.

For further refinement of our results, we studied the LR of each parameter. The LR is the likelihood that a given parameter (test) result would be expected in a patient with the disease compared to the likelihood that that same result would be expected in a patient without the disease.[12] In other words, the LR indicates how much a given diagnostic test result will raise or lower the pretest probability of the disease in question.[11] We found that GC-IPL parameters outperformed the RNFL with higher positive LR, that is, lower values of inferior and inferotemporal sector helped in ruling in the disease. Not much could be gained from the negative LR values.

Average thickness on RNFL has been considered to be of more diagnostic value than average thickness on GC-IPL. We

Table 4: Likelihood ratios for positive and negative test results (with 95% CI) of ONH, RNFL, and GCIPL parameters

	Diagnostic indicators	
	LR+ (95% CI)	LR- (95% CI)
ONH parameters		
Rim area	3.19 (1.85-5.51)	0.50 (0.37-0.68)
Average CDR	2.21 (1.55-3.13)	0.34 (0.21-0.54)
Vertical CDR	2.95 (1.88-4.62)	0.36 (0.24-0.54)
Cup volume	1.67 (1.28-2.18)	0.35 (0.20-0.61)
RNFL parameters		
Clock hour_1	2.00 (1.33-3.01)	0.55 (0.40-0.77)
Clock hour_2	2.10 (1.13-3.91)	0.77 (0.63-0.95)
Clock hour_3	2.82 (1.20-6.63)	0.81 (0.70-0.95)
Clock hour_4	1.35 (0.96-1.89)	0.73 (0.52-1.04)
Clock hour_5	3.37 (2.08-5.47)	0.35 (0.24-0.52)
Clock hour_6	3.64 (2.06-6.43)	0.46 (0.34-0.63)
Clock hour_7	2.52 (1.66-3.84)	0.42 (0.28-0.61)
Clock hour_8	1.73 (1.34-2.23)	0.25 (0.13-0.48)
Clock hour_9	1.83 (1.20-2.77)	0.63 (0.47-0.86)
Clock hour_10	1.87 (1.40-2.5)	0.30 (0.17-0.52)
Clock hour_11	2.27 (1.53-3.37)	0.44 (0.30-0.64)
Clock hour_12	3.29 (1.97-5.49)	0.43 (0.30-0.60)
Temporal quadrant	1.36 (0.88-2.10)	0.83 (0.64-1.08)
Superior quadrant	2.34 (1.68-3.25)	0.22 (0.12-0.40)
Nasal quadrant	2.25 (1.58-3.18)	0.32 (0.20-0.52)
Inferior quadrant	2.59 (1.82-3.68)	0.19 (0.10-0.35)
Average thickness	2.41 (1.74-3.35)	0.17 (0.09-0.34)
GCIPL parameters		
Superotemporal sector	3.12 (1.68-5.78)	0.62 (0.48-0.78)
Superior sector	2.14 (1.43-3.19)	0.49 (0.35-0.71)
Superonasal sector	2.56 (1.62-4.06)	0.49 (0.35-0.68)
Inferonasal sector	4.20 (1.99-8.83)	0.61 (0.49-0.77)
Inferior sector	4.90 (2.19-10.93)	0.60 (0.48-0.75)
Inferotemporal sector	5.19 (2.34-11.55)	0.57 (0.45-0.72)
Average thickness	4.23 (2.13-8.39)	0.55 (0.42-0.71)
Minimum thickness	2.54 (1.53-4.23)	0.58 (0.43-0.76)

LR=Likelihood ratio

found that these averages though had an AUC of 0.63 and 0.69, respectively; the former had high sensitivity at 89.04 with poor specificity (63.08) and the latter had low sensitivity (52.05) and high specificity (87.69). Interestingly, we found that the average RNFL thickness had low positive and negative LR, whereas, average GC-IPL had higher positive LR. This implies that lower the latter's value; more is the likelihood of the disease being present. Na *et al.*, have noted that the nasal and temporal sides of the optic disc (where early glaucomatous change is rare) are included in the analysis, which may reduce the sensitivity of glaucoma detection if average RNFL thickness is considered.[4]

The AUCs of RNFL parameters have been shown to have more diagnostic values than GC-IPL parameters.[4,5,11] However, on further analysis using LR; the likelihood of ruling in and/or ruling out a disease favored the GC-IPL parameters. Harsha *et al.* showed that the likelihood of having the disease was highest for inferior GCC when PPG eyes were compared to glaucoma suspects.[11] They also reported that when the controls were relaxed to normal eyes, the highest LR was seen with inferior RNFL. Our study differs in reporting the GC-IPL inferotemporal sector to be the best performer.

Begum *et al.* reported that ONH, RNFL, and GC-IPL parameters were, respectively, associated with large, moderate, and no effects on the posttest probability of PPG.[9] It is important to note that these effects, though small, still can become relevant and useful, depending on other clinical information and the pretest probability of disease.[9]

Our findings are also contrary to another recent study in Indian population, wherein it was concluded that GCA measurements, as provided by the SD-OCT, do not appear to outperform RNFL measurements in the diagnosis of PPG.[10] However, this study group comprised ocular hypertensives and glaucoma suspects. The results may have differed due to different definition of PPG in both the studies.

It has been noted that RGCs are selectively lost early in glaucoma.[13] More than 50% of all RGCs are concentrated and multilayered in the macular area.[5] Zeimer *et al.* hypothesized that quantitative detection of glaucomatous damage at the posterior pole using retinal thickness mapping may provide a unique method for the early detection and monitoring of early glaucomatous tissue loss.[14] There have been studies, which have reported better diagnostic values with macular scans than RNFL.[15] However, it is important to note that the study group was derived from a population known to have larger prevalence of normal-tension glaucoma where defects are closer to fixation and hence to fovea. As GC-IPL parameters were computed from the data of a restricted scan area (i.e., an elliptical annulus centered on the fovea), the sensitivity for detecting RGC loss might be affected by where the RGC loss is mostly located.[13]

Comparable diagnostic capability of GC-IPL to that of RNFL thickness measurements has been reported for PPG.[16,17] Kim *et al.* reported that the inner directional angle of RNFL defects affected the diagnostic sensitivity of macular GC-IPL parameters.[18] Recently it has been found that significantly lower RNFL and GCC measurements were present in normal looking discs of individuals with a history of POAG in their first-degree relatives, compared to individuals without a similar history.[16] Lee and associates, found that inferotemporal thickness on GC-IPL had the best AUC in a study comprising wide field RNFL maps in eyes with PPG.[19] Inuzuka studied 77 eyes of PPG and reported that GC-IPL thicknesses in the inferior and inferotemporal sectors might serve as useful parameters to track the progression of glaucomatous changes in eyes with PPG.[20] Kim and associates recently reported that segmented IPL thickness is significantly associated with the degree of glaucoma.[21] In PPG group, the structure-function relationship of the GCL, IPL, and GCIPL thickness is stronger than the RNFL thickness.

Limitations

This study has certain limitations. PPG was diagnosed clinically by two glaucoma specialists and was based on normal VF results in the presence of one or more localized RNFL defects that were associated with a glaucomatous disc appearance. It cannot be stated with a degree of certainty that few of the study eyes may have been normal physiological variants as reported previously.[11] Medeiros *et al.* therefore have recommended longitudinal evaluation of optic discs for detecting change and definitively diagnosing PPG.[22] Our control group comprised of true normals. Differentiation between PPG and a normal eye is easier as compared to a glaucoma suspect. However, adding

suspects in our study would have reduced the specificity and including true normals improved our sensitivity.

The sample size of our study group is small and large population-based studies are required for generalization of the results. Our results may not be applicable to individuals with low-tension glaucoma as only eyes with IOP >21 mmHg were included. There are studies that have shown that RNFL and GCC reduce with increased axial length and negative spherical equivalent; hence, we excluded eyes with refractive errors outside −6DS and +4DS.[23] Our results may not be applicable to eyes falling beyond our criterion. These limitations must be taken into account when interpreting OCT results in PPG.

Conclusion

We studied structural parameters in PPG and found that diagnostic ability of RNFL parameters was comparable to GC-IPL. But the likelihood of ruling in a disease was greater with GC-IPL.

Financial support and sponsorship

Nil.

Conflicts of interest

There are no conflicts of interest.

References

1. Quigley HA, Addicks EM, Green WR. Optic nerve damage in human glaucoma. III. Quantitative correlation of nerve fiber loss and visual filed defect in glaucoma, ischemic neuropathy, papilledema, and toxic neuropathy. Arch Ophthalmol 1982;100:135-46.
2. Quigley HA, Dunkelberger GR, Green WR. Retinal ganglion cell atrophy correlated with automated perimetry in human eyes with glaucoma. Am J Ophthalmol 1989;107:453-64.
3. Asaoka R, Iwase A, Hirasawa K, Murata H, Araie M. Identifying ''preperimetric'' glaucoma in standard automated perimetry visual fields. Invest Ophthalmol Vis Sci 2014;55:7814-20.
4. Na JH, Sung KR, Baek SH, Kim ST, Shon K, Jung JJ. Rates and patterns of macular and circumpapillary retinal nerve fiber layer thinning in preperimetric and perimetric glaucomatous eyes. J Glaucoma 2015;24:278-85.
5. Deshpande GA, Bawankule PK, Raje DV, Chakraborty M. Linear discriminant score for differentiating early primary open angle glaucoma from glaucoma suspects. Indian J Ophthalmol 2019;67:75-81.
6. Nassif N, Cense B, Park BH, Yun SH, Chen TC, Bouma BE, *et al. In vivo* human retinal imaging by ultrahigh-speed spectral-domain optical coherence tomography. Opt Lett 2004;29:480-2.
7. Nouri-Mahdavi K, Nowroozizadeh S, Nassiri N, Cirineo N, Knipping S, Giaconi J, *et al*. Macular ganglion cell/inner plexiform layer measurements by spectral domain optical coherence tomography for detection of early glaucoma and comparison to retinal nerve fiber layer measurements. Am J Ophthalmol 2013;156:1297-307.
8. Lisboa R, Paranhos A Jr, Weinreb RN, Zangwill LM, Leite MT, Medeiros FA. Comparison of different spectral domain OCT scanning protocols for diagnosing preperimetric glaucoma. Invest Ophthalmol Vis Sci 2013;54:3417-25.
9. Begum VU, Addepalli UK, Yadav RK, Shankar K, Senthil S, Garudadri CS, *et al*. Ganglion cell-inner plexiform layer thickness of high definition optical coherence tomography in perimetric and preperimetric glaucoma. Invest Ophthalmol Vis Sci 2014;55:4768-75.
10. Kaushik S, Kataria P, Jain V, Joshi G, Raj S, Pandav SS. Evaluation of macular ganglion cell analysis compared to retinal nerve fiber layer thickness for preperimetric glaucoma diagnosis. Indian J Ophthalmol 2018;66:511-6.
11. Rao HL, Addepalli UK, Chaudhary S, Kumbar T, Senthil S, Choudhari NS, *et al*. Ability of different scanning protocols of spectral domain optical coherence tomography to diagnose preperimetric glaucoma. Invest Ophthalmol Vis Sci 2013;54:7252-7.
12. Biggerstaff BJ. Comparing diagnostic tests: A simple graphic using likelihood ratios, Stat Med 2000;19:649-63.
13. Zeimer R, Asrani S, Zou S, Quigley H, Jampel H. Quantitative detection of glaucomatous damage at the posterior pole by retinal thickness mapping. A pilot study. Ophthalmology 1998;105:224-31.
14. Barua N, Sitaraman C, Goel S, Chakraborti C, Mukherjee S, Parashar H. Comparison of diagnostic capability of macular ganglion cell complex and retinal nerve fiber layer among primary open angle glaucoma, ocular hypertension, and normal population using Fourier-domain optical coherence tomography and determining their functional correlation in Indian population. Indian J Ophthalmol 2016;64:296-302.
15. Na JH, Sung KR, Baek S, Kim YJ, Durbin MK, Lee HJ, *et al*. Detection of glaucoma progression by assessment of segmented macular thickness data obtained using spectral domain optical coherence tomography. Invest Ophthalmol Vis Sci 2012;53:3817-26.
16. Karti O, Yuksel B, Uzunel UD, Karahan E, Zengin MO, Kusbeci T. The assessment of optical coherence tomographic parameters in subjects with a positive family history of glaucoma. Clin Exp Optom 2017;100:663-7.
17. Jung Y, Park HY, Jeong HJ, Choi SY, Park CK. The ability of 10-2 short-wavelength perimetry in detecting functional loss of the macular area in preperimetric glaucoma patients. Invest Ophthalmol Vis Sci 2015;56:7708-14.
18. Kim MJ, Jeoung JW, Park KH, Choi YJ, Kim DM. Topographic profiles of retinal nerve fiber layer defects affect the diagnostic performance of macular scans in preperimetric glaucoma. Invest Ophthalmol Vis Sci 2014;55:2079-87.
19. Lee WJ, Na KI, Kim YK, Jeoung JW, Park KH. Diagnostic ability of wide-field retinal nerve fiber layer maps using swept-source optical coherence tomography for detection of preperimetric and early perimetric glaucoma. J Glaucoma 2017;26:577-85.
20. Inuzuka H, Kawase K, Sawada A, Kokuzawa S, Ishida K, Yamamoto T. Development of glaucomatous visual field defects in preperimetric glaucoma patients within 3 years of diagnosis. J Glaucoma 2016;25:e591-5.
21. Kim EK, Park HL, Park CK. Segmented inner plexiform layer thickness as a potential biomarker to evaluate open-angle glaucoma: Dendritic degeneration of retinal ganglion cell. PLoS One 2017;12:e0182404.
22. Medeiros FA, Zangwill LM, Bowd C, Weinreb RN. Comparison of the GDx VCC scanning laser polarimeter, HRT II confocal scanning laser ophthalmoscope, and stratus OCT optical coherence tomograph for the detection of glaucoma. Arch Ophthalmol 2004;122:827-37.
23. Mwanza JC, Oakley JD, Budenz DL, Chang RT, Knight OJ, Feuer WJ. Macular ganglion cell-inner plexiform layer: Automated detection and thickness reproducibility with spectral domain-optical coherence tomography in glaucoma. Invest Ophthalmol Vis Sci 2011;52:8323-9.